ISA Transactions 53 (2014) 1332–1342

Contents lists available at ScienceDirect

ISA Transactions

journal homepage: www.elsevier.com/locate/isatrans

Research Article

Guidance law against maneuvering targets with intercept angle constraint

Shaofeng Xiong [a,b,*], Weihong Wang [a,b], Xiaodong Liu [c,d], Sen Wang [a,b], Zengqiang Chen [e]

[a] School of Automation Science and Electrical Engineering, Beijing University of Aeronautics & Astronautics, Beijing 100191, China
[b] Science and Technology on Aircraft Control Laboratory, Beijing University of Aeronautics & Astronautics, Beijing 100191, China
[c] Beijing Aerospace Automatic Control Institute, Beijing 100854, China
[d] National Key Laboratory of Science and Technology on Aerospace Intelligence Control, Beijing 100854, China
[e] Department of Automation, Nankai University, Tianjin 300071, China

ARTICLE INFO

Article history:
Received 24 November 2013
Received in revised form
4 March 2014
Accepted 21 March 2014
Available online 26 April 2014
"This paper was recommended for publication by Jeff Pieper".

Keywords:
Nonlinear guidance law
Maneuvering target
Intercept angle constraint
Extended state observer
Sliding mode control

ABSTRACT

This study explores the guidance law against maneuvering targets with the intercept angle constraint. The limitation of the traditional guidance law, which simply treats the unknown target acceleration as zero, has been analyzed. To reduce this limitation, a linear extended state observer is constructed to estimate the acceleration of the maneuvering target to enhance the tracking performance of the desired intercept angle. Furthermore, a nonsingular terminal sliding mode control scheme is adopted to design the sliding surface, which is able to avoid the singularity in the terminal phase of guidance. Simulation results have demonstrated that the proposed guidance law outperforms the traditional guidance law in the sense that more accurate intercept angle can be achieved.

1. Introduction

In order to increase the lethality of the missile's warhead against targets such as new large aircrafts, modern warships, submarines, tanks and large buildings, not only obtaining accurate interception with the target, but also striking the target at a desired intercept angle would be required. There is currently a vast literature on the design of intercept angle guidance law (IAGL), accumulated over more than four decades of investigations. In the early stage, traditional proportional navigation guidance law and its variants were employed to satisfy impact angle constraint [1–4]. Afterwards, optimal control theory was exploited to construct IAGL [5–7].

Thanks to the robustness to highly nonlinear dynamic systems with large modeling errors and external disturbance [8], the sliding mode control (SMC) technique had been employed for the design of guidance law [9–12]. In [13], the traditional linear SMC methodology was used to derive IAGL which enables intercepting a maneuvering target in three kinds of interception geometries, i.e., head-on, tail-chase and novel head pursuit. In [13], the information of the target acceleration was necessary for constructing the sliding variable, while no information was given about how to get the target acceleration in the simulation section. The guidance law in [13] can only guarantee asymptotic stability, and the investigations on the finite-time convergent IAGL had been proposed in [14–18]. With the help of the technique of line of sight (LOS) rate shaping, a finite-time convergent impact time and angle guidance law for stationary or constant velocity targets was proposed in [14] by the use of the second order SMC algorithm. In [15,17], the traditional terminal sliding mode (TSM) control algorithm was employed to construct a sliding variable to satisfy the intercept angle constraint. Furthermore in [16], considering a first-order-lag autopilot, an integral sliding mode controller combining nonlinear disturbance observer was developed to derive a novel composite IAGL. Both of the guidance laws in [15,16] defined the LOS angle as the intercept angle.

Different from the guidance laws in [15,16], the intercept angle in [17,18] was defined as the angle between the velocity vectors of the missile and the target when the interception occurs. For a given intercept angle, whether or not the target is maneuvering, the desired LOS angle is constant and its first time derivative is zero under the definition of intercept angle proposed in [15,16]. Comparatively, under the definition of intercept angle proposed in literatures [17,18], it holds only when the target executes no maneuver. The desired LOS angle is time-varying and its first time derivative is proportional to the target acceleration when the

* Corresponding author at: School of Automation Science and Electrical Engineering, Beijing University of Aeronautics & Astronautics, XueYuan Road No. 37, HaiDian District, Beijing 100191, China.
E-mail address: 15210985746@163.com (S. Xiong).

http://dx.doi.org/10.1016/j.isatra.2014.03.007
0019-0578/

target executes maneuvering. Both guidance laws in literatures [15,17] performed well for intercepting stationary and constant velocity targets. Especially, the guidance law proposed in [17] could steer the missile to intercept the stationary and constant velocity targets at all-aspect impact angle with different initial heading angles. However, in the case of intercepting maneuvering targets, the desired LOS angle is time-varying and its first time derivative is no longer zero but proportional to the target acceleration. So in [17], the target acceleration was included in the designed terminal sliding variable when target executes maneuvering. As pointed out in [17], it was usually difficult to measure the target acceleration directly in practice, and the target acceleration was treated as an unknown bounded variable. It is important to deal with the problem of unknown target acceleration when calculating the designed terminal sliding surface. Unfortunately, in the simulation of intercepting maneuvering targets, the literature [17] did not explain how to deal with the unknown target acceleration which was crucial for implementing the proposed IAGL. In addition, both of the guidance laws in [15,17] suffered from the problem of singularity. The literature [18] proposed a nonsingular terminal sliding mode (NTSM) control scheme based IAGL which was only suitable for non-maneuvering targets.

To handle the problem of the unknown target acceleration when intercepting maneuvering targets, an ingenious missile guidance law was proposed in [19]. In literature [19], the guidance design consisted of the estimation of the target acceleration by extended state observer (ESO) and achieved the decrease of undesired chattering effectively. However, only the problem of missile interception was investigated and the intercept angle constraint was not considered in [19]. In another method, the unknown target acceleration was directly set to zero. Setting the unknown target acceleration to zero is equivalent to letting the first time derivative of the desired LOS angle be zero. On the one hand, setting the first time derivative of the desired LOS angle to zero means that the first time derivative of the LOS angle should track zero, which is equivalent to rendering the LOS angle changeless in guidance. On the other hand, the LOS angle is required to track the time-varying desired LOS angle when the target executes maneuvering. The discrepancy of these two requirements poses a serious challenge for the LOS angle to precisely track the time-varying desired LOS angle when the target executes maneuvering, and furthermore gives rise to poor performance in obtaining the desired intercept angle.

As discussed above, under the definition of the intercept angle proposed in [17], how to deal with the unknown target acceleration has become the key problem in achieving higher tracking precision of the desired intercept angle for intercepting maneuvering targets. Other than simply setting the unknown target acceleration to zero, in this paper we treat it as an augmented state and estimate it by using a linear extended state observer (LESO) which is easier to implement. Due to the robustness and simplicity of LESO, an accurate estimation of the unknown target acceleration can be obtained. Different from the guidance law in [19], where the estimation of the unknown target acceleration was used to make the disturbance compensation in the control input and then reduce the chattering and control power, while in this paper it is used to calculate the designed nonsingular terminal sliding variable which satisfies the intercept angle constraint. With the accurate estimation of the unknown target acceleration, thus the time-varying desired LOS angle can be tracked accurately when the target executes maneuvering, which guarantees higher tracking precision of the desired intercept angle. To the authors' knowledge, under the definition of the intercept angle proposed in [17], no NTSM algorithm based IAGL for intercepting maneuvering targets has ever appeared in previously published literatures. So no need to set the unknown target acceleration to zero and singularity-free when attacking maneuvering targets with intercept angle constraint are the main contributions that set this work apart from other literatures.

The rest of this paper is organized as follows. The equations of engagement geometry and the definition of intercept angle are given in Section 2. The SMC and ESO algorithms are introduced in Section 3. In Section 4, the IAGL for intercepting maneuvering targets is proposed based on NTSM and LESO methods. In Section 5, numerical simulations are implemented for both setting the unknown target acceleration to zero and our proposed guidance law to justify the superiority of our proposed IAGL. Conclusions are given in Section 6.

2. Geometry of engagement

In this section, a two-dimensional engagement geometry involving missile and target is considered. To simplify the design, some assumptions are adopted that both of the missile and the target are viewed as point mass and the dynamics of autopilot and actuator are fast enough to be neglected. The interception geometry is shown in Fig. 1. The corresponding relative kinematic equations between the missile and the target in polar coordinate form are as follows:

$$\dot{r} = V_T \cos(\phi_T - \lambda) - V_M \cos(\phi_M - \lambda) \tag{1}$$

$$\dot{\lambda} = \frac{V_T \sin(\phi_T - \lambda) - V_M \sin(\phi_M - \lambda)}{r} \tag{2}$$

$$\dot{\phi}_M = \frac{A_M}{V_M} \tag{3}$$

$$\dot{\phi}_T = \frac{A_T}{V_T} \tag{4}$$

where λ denotes the LOS angle, r denotes the distance between the missile and the target, A_M, ϕ_M, V_M, A_T, ϕ_T and V_T denote the normal accelerations, the heading angles and the tangential velocities of the missile and the target, respectively. Both V_M and V_T are assumed to be constant during the entire process of guidance. Here, two variables are defined as

$$V_r = \dot{r} \tag{5}$$

$$V_\lambda = r\dot{\lambda} \tag{6}$$

where V_r and V_λ represent relative velocities along and perpendicular to the LOS between the missile and the target respectively.

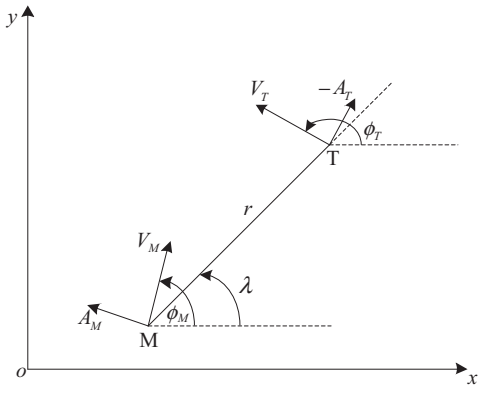

Fig. 1. Missile target engagement geometry.

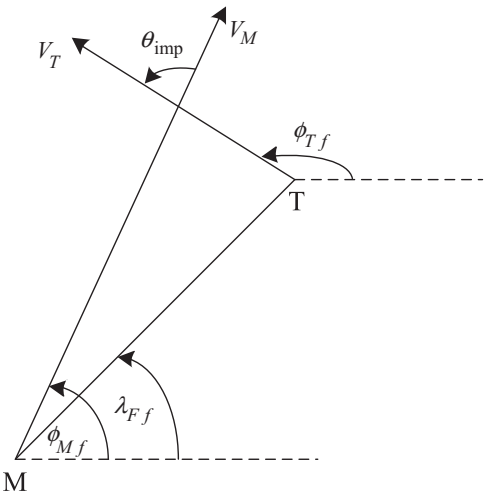

Fig. 2. Missile and target on collision course.

Differentiating Eqs. (2) and (6) with respect to time and substituting Eqs. (1) and (3)–(5) into them yields

$$\ddot{\lambda} = -\frac{2\dot{r}\dot{\lambda}}{r} + \frac{A_{T\lambda}}{r} - \frac{\cos(\phi_M - \lambda)}{r} A_M \tag{7}$$

$$\dot{V}_\lambda = -V_r\dot{\lambda} + A_{T\lambda} - A_M \cos(\phi_M - \lambda) \tag{8}$$

where $A_{T\lambda} = A_T \cos(\phi_T - \lambda)$ is projection of the target acceleration which is perpendicular to the LOS. These two equations are very important for the design of subsequent IAGL. In practical scenario, it is usually difficult to measure the target acceleration A_T directly, so A_T and $A_{T\lambda}$ are commonly treated as unknown variables. In this paper, $A_{T\lambda}$ is viewed as an augmented state and estimated by the LESO. Then the estimation of the target acceleration A_T can be obtained, which plays a key role in the proposed IAGL construction.

As shown in Fig. 2, when interception occurs, the impact angle is defined as

$$\theta_{imp} = \phi_{Tf} - \phi_{Mf} \tag{9}$$

where ϕ_{Tf} and ϕ_{Mf} are the heading angles of the target and the missile respectively when interception occurs. When the missile and the target are on collision course, the relative speed perpendicular to the LOS is zero, it follows

$$V_M \sin(\phi_{Mf} - \lambda_{Ff}) - V_T \sin(\phi_{Tf} - \lambda_{Ff}) = 0 \tag{10}$$

It is assumed that $V_T < V_M$, so it yields

$$\lambda_{Ff} = \phi_{Tf} - \tan^{-1}\left(\frac{\sin\theta_{imp}}{\cos\theta_{imp} - V_T/V_M}\right) \tag{11}$$

where λ_{Ff} represents the desired LOS angle when interception occurs. Eq. (11) expresses the relationship between the desired LOS angle λ_F and the target's flight path angle ϕ_T when interception occurs. In order to obtain the desired impact angle θ_{imp} when interception occurs, a feasible method is to establish Eq. (11) from the beginning of guidance. So Eq. (11) can be rewritten as the following form:

$$\lambda_F = \phi_T - \tan^{-1}\left(\frac{\sin\theta_{imp}}{\cos\theta_{imp} - V_T/V_M}\right) \tag{12}$$

Due to the property of maneuverability, the target's heading angle ϕ_T changes with time. So according to Eq. (12), the desired LOS angle λ_F is also time-varying and its first time derivative is proportional to the target acceleration A_T. The first and second time derivatives of the desired LOS angle λ_F are

$$\dot{\lambda}_F = \dot{\phi}_T = A_T/V_T, \quad \ddot{\lambda}_F = \ddot{\phi}_T = \dot{A}_T/V_T. \tag{13}$$

3. Sliding-mode control and extended state observer

In this part, some types of TSM control algorithm and the ESO theory will be introduced.

The TSM and NTSM control schemes can be described by the following first-order nonlinear differential equations [20,21]

$$s = \dot{x} + \alpha|x|^\eta sign(x) = 0 \tag{14}$$

$$s = x + \beta|\dot{x}|^\gamma sign(\dot{x}) = 0 \tag{15}$$

respectively, where $x \in R$, $\alpha, \beta > 0$, $0 < \eta < 1$, $1 < \gamma < 2$. The NTSM control method (15) is equivalent to the conventional TSM control scheme (14) as

$$s = \dot{x} + \beta'|x|^{\gamma'} sign(x) = 0, \quad \beta' = \beta^{-1/\gamma} > 0, \quad \frac{1}{2} < \gamma' = \frac{1}{\gamma} < 1 \tag{16}$$

Remark 1. The zero solution $x = 0$ of Eqs. (14) and (15) are both globally finite-time stable and the system state converges to the equilibrium point $x = 0$ from any specified initial state $x(0) = x_0$ within the time

$$T_t = \frac{1}{\alpha(1-\eta)}|x_0|^{1-\eta} \tag{17}$$

$$T_{nt} = \frac{\beta^{1/\gamma}|x_0|^{1-1/\gamma}}{1-1/\gamma} \tag{18}$$

respectively.

Remark 2. The TSM function (14) and NTSM function (15) are both continuous and differentiable although they include the absolute value and signum operator. Differentiating (14) and (15) with respect to time respectively, then it yields that

$$\dot{s} = \ddot{x} + \alpha\eta|x|^{\eta-1}\dot{x} \tag{19}$$

$$\dot{s} = \dot{x} + \beta\gamma|\dot{x}|^{\gamma-1}\ddot{x} \tag{20}$$

Due to $-1 < \eta - 1 < 0$, thus $|x|^{\eta-1} \to \infty$ as $x \to 0$. So consider the control design, the conventional TSM method (14) suffers from the problem of singularity. Meanwhile, as can be seen from (20) that, because $0 < \gamma - 1 < 1$, so $|\dot{x}|^{\gamma-1} \to 0$ as $\dot{x} \to 0$, then Eq. (15) is singularity-free.

The ESO was originally proposed by Han [22–24]. The proofs of convergence for ESO in linear and nonlinear cases are first provided in [25,26] and [27] respectively. The main advantage of ESO is that it can estimate the internal system state variables and external disturbance simultaneously in the absence of an accurate mathematical model of the plant. The ESO in its original form employs nonlinear observer gains. The LESO with one tuning parameter was proposed in [28–30], which simplified the ESO's implementation and made the design transparent to engineers. Using the partially known modeling information of the plant, the alternative active disturbance rejection control (ADRC) was applied to the MEMS electrostatic actuator in [31]. In our research, only the target acceleration is unknown and other parameters are assumed known. So the LESO in alternative ADRC is introduced here.

Consider the following first order controlled plant:

$$\dot{x} = f(x) + v(t) + bu(t) \tag{21}$$

where $f(x)$ represents the internal dynamics of the plant and is assumed known, $v(t)$ denotes the unknown external disturbance, $u(t)$ denotes the control input and x denotes the output. Designating x as x_1 and $v(t)$ as an augmented state x_2, then Eq. (21) can be extended to a new second order dynamic system

$$\begin{aligned} \dot{x}_1 &= x_2 + f(x) + bu(t) \\ \dot{x}_2 &= h \end{aligned} \tag{22}$$

where $h=\dot{v}$ represents the rate of change of $v(t)$ and is assumed to be an unknown bounded function. In order to estimate the value of $v(t)$, consider the following second order LESO:

$$\begin{aligned}\dot{z}_1 &= z_2-\beta_{01}e_1+f(x)+bu(t)\\ \dot{z}_2 &= -\beta_{02}e_1\end{aligned} \tag{23}$$

where $e_1=z_1-x_1$, $\beta_{01}=2\omega_0>0$, $\beta_{02}=\omega_0^2>0$ and ω_0 denotes the bandwidth of the observer. If appropriate value is selected for ω_0, then the estimated variables z_1 and z_2 will intend converging to x_1 and x_2 respectively.

4. Guidance law design

In order to avoid the problem of singularity in guidance, the NTSM control scheme described in Eq. (15) is employed to design the sliding manifold. Consider intercepting a maneuvering target, it can be observed from Eq. (13) that the first time derivative of the desired LOS angle is proportional to the target acceleration. So the target acceleration is necessary for constructing the sliding surface. It is usually difficult to measure the target acceleration directly, so the target acceleration is designated as an augmented state and estimated by using LESO.

Considering dynamic system (7) with the relative degree of two between the missile acceleration A_M and the LOS angle λ, we rewrite it as follows:

$$\ddot{\lambda}=-\frac{2\dot{r}\dot{\lambda}}{r}+\frac{A_{T\lambda}}{r}-\frac{\cos(\phi_M-\lambda)}{r}A_M \tag{24}$$

It can be observed from Eq. (24) that the LOS angle λ can be controlled for all $|\phi_M-\lambda|\neq\pi/2$. Also in literature [17] it has been justified that $|\phi_M-\lambda|=\pi/2$ is not a stable equilibrium due to $\dot{\phi}_M-\dot{\lambda}\neq 0$ when $|\phi_M-\lambda|=\pi/2$, therefore the missile acceleration A_M can be employed to control the LOS angle λ to track the desired LOS angle λ_F defined in Eq. (12).

As usual in SMC design, the first step is to construct a sliding surface which guarantees achievement of the desired control requirements. According to the NTSM control algorithm described in (15), the following sliding surface is developed:

$$s=(\lambda-\lambda_F)+\beta|\dot{\lambda}-\dot{\lambda}_F|^{\gamma}sign(\dot{\lambda}-\dot{\lambda}_F) \tag{25}$$

where $\beta>0$, $1<\gamma<2$, λ_F denotes the desired LOS angle. It is evident that the sliding surface (25) creates the finite-time convergence of $\lambda-\lambda_F$ from initial state $\lambda_0'-\lambda_{F0}'$ to zero without singularity. Here the initial state $\lambda_0'-\lambda_{F0}'$ denotes state when the sliding motion (25) occurs.

Substituting Eq. (13) into Eq. (25) yields

$$s=(\lambda-\lambda_F)+\beta\left|\dot{\lambda}-\frac{A_T}{V_T}\right|^{\gamma}sign\left(\dot{\lambda}-\frac{A_T}{V_T}\right) \tag{26}$$

Differentiating Eq. (26) with respect to time, it follows

$$\dot{s}=\left(\dot{\lambda}-\frac{A_T}{V_T}\right)+\beta\gamma\left|\dot{\lambda}-\frac{A_T}{V_T}\right|^{\gamma-1}\left(\ddot{\lambda}-\frac{\dot{A}_T}{V_T}\right) \tag{27}$$

Substituting Eq. (24) into Eq. (27) and designating $\dot{s}$ to zero, then the equivalent controller can be depicted in the following form:

$$A_{Meq}=\frac{r}{\cos(\phi_M-\lambda)}\left[\frac{1}{\beta\gamma}\left|\dot{\lambda}-\frac{A_T}{V_T}\right|^{2-\gamma}sign\left(\dot{\lambda}-\frac{A_T}{V_T}\right)-\frac{2\dot{r}\dot{\lambda}}{r}+\frac{A_{T\lambda}}{r}-\frac{\dot{A}_T}{V_T}\right] \tag{28}$$

Consider the constant rate reaching law, so the control input can be described as

$$A_M=\frac{r}{\cos(\phi_M-\lambda)}\left[\frac{1}{\beta\gamma}\left|\dot{\lambda}-\frac{A_T}{V_T}\right|^{2-\gamma}sign\left(\dot{\lambda}-\frac{A_T}{V_T}\right)-\frac{2\dot{r}\dot{\lambda}}{r}+\frac{A_{T\lambda}}{r}-\frac{\dot{A}_T}{V_T}+\frac{\eta sign(s)}{r}\right] \tag{29}$$

where the sliding gain $\eta>0$. It can be seen that those unknown variables A_T, $A_{T\lambda}$ and $\dot{A}_T$ are included in Eqs. (26) and (29), therefore the information of the target acceleration is necessary for implementing the proposed guidance law. Here the estimation of $A_{T\lambda}$ can be obtained by the LESO. Dividing it by $\cos(\phi_T-\lambda)$ yields the estimation of A_T.

Designating $A_{T\lambda}$ as an augmented state, then Eq. (8) can be extended to a new second order dynamic system

$$\begin{aligned}\dot{V}_\lambda &= A_{T\lambda}-V_r\dot{\lambda}-A_M\cos(\phi_M-\lambda)\\ \dot{A}_{T\lambda} &= h\end{aligned} \tag{30}$$

where h is the first time derivative of $A_{T\lambda}$, $-V_r\dot{\lambda}$ denotes the partially known information of the system. According to Eq. (23), the second order LESO for system (30) is constructed as

$$\begin{cases}\dot{z}_1=z_2-\beta_{01}e_1-V_r\dot{\lambda}-A_M\cos(\phi_M-\lambda)\\ \dot{z}_2=-\beta_{02}e_1\\ \beta_{01}=2\omega_0\\ \beta_{02}=\omega_0^2\end{cases} \tag{31}$$

where $e_1=z_1-V_\lambda$ is the estimation error of V_λ, ω_0 is the bandwidth of the observer, z_1 and z_2 are estimations of V_λ and $A_{T\lambda}$ respectively. Via tuning the parameter ω_0 properly, then z_1 and z_2 will converge to V_λ and $A_{T\lambda}$ respectively. The estimation of $A_{T\lambda}$ is obtained by the LESO (31) firstly. Then, the estimation of the target acceleration A_T can be described as

$$A_T=\frac{A_{T\lambda}}{\cos(\phi_T-\lambda)}=\frac{z_2}{\cos(\phi_T-\lambda)} \tag{32}$$

Therefore in the execution of the proposed guidance law, the sliding manifold in Eq. (26) can be modified as

$$s=(\lambda-\lambda_F)+\beta\left|\dot{\lambda}-\frac{z_2}{\cos(\phi_T-\lambda)V_T}\right|^{\gamma}sign\left(\dot{\lambda}-\frac{z_2}{\cos(\phi_T-\lambda)V_T}\right) \tag{33}$$

with A_T and $A_{T\lambda}$ estimated by the LESO, and $\dot{A}_T$ is treated as unknown bounded disturbance, hence the control input described in Eq. (29) can be modified as

$$\begin{aligned}A_{MESO}=\frac{r}{\cos(\phi_M-\lambda)}\Bigg[&\frac{1}{\beta\gamma}\left|\dot{\lambda}-\frac{z_2}{\cos(\phi_T-\lambda)V_T}\right|^{2-\gamma}\\ &sign\left(\dot{\lambda}-\frac{z_2}{\cos(\phi_T-\lambda)V_T}\right)-\frac{2\dot{r}\dot{\lambda}}{r}+\frac{z_2}{r}+\frac{\eta sign(s)}{r}\Bigg]\end{aligned} \tag{34}$$

To determine the bound on sliding gain η of reaching law, consider the following Lyapunov function candidate:

$$V=\tfrac{1}{2}s^2 \tag{35}$$

Taking the first time derivative of Eq. (35) and substituting Eqs. (27) and (34) into it, we obtain

$$\begin{aligned}\dot{V}&=s\Bigg[\dot{\lambda}-\frac{A_T}{V_T}+\beta\gamma\left|\dot{\lambda}-\frac{A_T}{V_T}\right|^{\gamma-1}\Bigg(\frac{A_{T\lambda}-z_2}{r}-\frac{\dot{A}_T}{V_T}-\frac{1}{\beta\gamma}\\ &\quad\left|\dot{\lambda}-\frac{z_2}{\cos\theta_T V_T}\right|^{2-\gamma}sign\left(\dot{\lambda}-\frac{z_2}{\cos\theta_T V_T}\right)-\frac{\eta sign(s)}{r}\Bigg)\Bigg]\\ &=s\Bigg[\dot{\lambda}-\frac{A_T}{V_T}+\beta\gamma\left|\dot{\lambda}-\frac{A_T}{V_T}\right|^{\gamma-1}\Bigg(\frac{A_{T\lambda}-z_2}{r}-\frac{\dot{A}_T}{V_T}-\frac{1}{\beta\gamma}\\ &\quad\left|\dot{\lambda}-\frac{z_2}{\cos\theta_T V_T}\right|^{2-\gamma}sign\left(\dot{\lambda}-\frac{z_2}{\cos\theta_T V_T}\right)\Bigg)\Bigg]-\beta\gamma\left|\dot{\lambda}-\frac{A_T}{V_T}\right|^{\gamma-1}\frac{\eta|s|}{r}\end{aligned} \tag{36}$$

where $\theta_T=\phi_T-\lambda$. To ensure $\dot{V}$ to be negative definite, the sliding gain η of reaching law should satisfy inequality

$$\eta>\left|\frac{r}{\beta\gamma}\left(\left|\dot{\lambda}-\frac{A_T}{V_T}\right|^{2-\gamma}sign\left(\dot{\lambda}-\frac{A_T}{V_T}\right)-\left|\dot{\lambda}-\frac{z_2}{\cos\theta_T V_T}\right|^{2-\gamma}sign\left(\dot{\lambda}-\frac{z_2}{\cos\theta_T V_T}\right)\right)+A_{T\lambda}-z_2-\frac{r\dot{A}_T}{V_T}\right| \tag{37}$$

It can be observed from inequality (37) that due to $0<2-\gamma<1$, thus no negative fractional power term is included in equality (37), therefore η is finite. When z_2 converges to $A_{T\lambda}$, $z_2/\cos\theta_T$ will converge to A_T. So in this situation, inequality (37) will be reduced to a simple form

$$\eta>\left|\frac{r\dot{A}_T}{V_T}\right| \tag{38}$$

Remark 3. In this paper, the unknown target acceleration A_T is estimated by the LESO which enables the calculation of the designed sliding manifold (25). This is truly the key point in the implementation of the proposed IAGL.

Remark 4. No negative fractional power term appears in the derived guidance command (34). Therefore no singularity occurs in the whole process of guidance and a reasonable missile acceleration can be obtained.

Remark 5. In order to alleviate the chattering, the sliding gain of reaching law in guidance command (34) is changed according to

$$\eta=\begin{cases}k, & |s|\geq\varepsilon\\ \frac{k}{\Delta_\eta}, & |s|<\varepsilon\end{cases} \tag{39}$$

where ε is the boundary layer of the sliding surface, k satisfies the requirement on the sliding gain η defined in equality (37). The parameter $\Delta_\eta\geq 1$ should be chosen by imposing a tradeoff between the oscillation stems from chattering and the effectiveness to restrain interference.

To achieve continuous guidance command, the discontinuous function $sign(s)$ included in control law (34) is approximated by a continuous sigmoid function

$$sgmf(s)=\begin{cases}2\left(\frac{1}{1+\exp^{-as}}-\frac{1}{2}\right), & |s|\leq\varepsilon\\ sign(s), & |s|>\varepsilon\end{cases} \tag{40}$$

where a is a constant that is inversely proportional to the boundary layer ε. In addition, although the target acceleration A_T is assumed to be bounded, but the estimation of the target acceleration $z_2/\cos(\phi_T-\lambda)$ diverges to infinite when $|\phi_T-\lambda|=(\pi/2)$, so the following saturation function is adopted:

$$\frac{z_2}{\cos\theta_T}=\begin{cases}A_{T\,max}sign\left(\frac{z_2}{\cos\theta_T}\right), & \left|\frac{z_2}{\cos\theta_T}\right|\geq A_{T\,max}\\ \frac{z_2}{\cos\theta_T}, & \text{others}\end{cases} \tag{41}$$

where $A_{T\,max}$ is the bound of the target acceleration.

Remark 6. As pointed out in [17], the presence of large heading errors, i.e., $\dot{r}>0$, may cause the proposed guidance law unable to steer the missile to the collision course and thus results in a miss. To solve this problem, the guidance law (34) is further changed into the following form:

$$A_{MESO}=\frac{1}{|\cos\theta_M|}\left[\frac{r}{\beta\gamma}\left|\dot{\lambda}-\frac{z_2}{\cos\theta_T V_T}\right|^{2-\gamma}sign\left(\dot{\lambda}-\frac{z_2}{\cos\theta_T V_T}\right)+2|\dot{r}|\dot{\lambda}+z_2+\eta sgmf(s)\right] \tag{42}$$

where $\theta_M=\phi_M-\lambda$ and $\theta_T=\phi_T-\lambda$. It can be observed from Eq. (42) that $A_{MESO}\to\infty$ when $|\theta_M|=\pi/2$, while this infinite large magnitude of acceleration cannot be provided by the missile in practice. Therefore in implementation, the actual missile acceleration given by (42) is clipped by the following saturation function:

$$A_{MESO}=\begin{cases}A_{M\,max}sign(A_{MESO}), & |A_{MESO}|\geq A_{M\,max}\\ A_{MESO}, & |A_{MESO}|<A_{M\,max}\end{cases} \tag{43}$$

where $A_{M\,max}$ is the limit of the missile acceleration.

5. Numerical simulations

In this section, numerical simulations are implemented for a variety of scenarios to illustrate the performance of the proposed IAGL. The initial conditions are as follows, the position of missile in inertial coordinate system is $x_{M0}=y_{M0}=0$ m, the distance between the missile and the target is $r_0=10{,}000$ m and the LOS angle is $\lambda_0=\pi/6$ rad. So the target's position in inertial coordinate system is $x_{T0}=8660.3$ m, $y_{T0}=5000$ m. The flight path angles and velocities of the missile and the target are $\phi_{M0}=\pi/4$ rad, $V_M=500$ m/s and $\phi_{T0}=2\pi/3$ rad, $V_T=250$ m/s, respectively. The intercept angle $\theta_{imp}=\pi/2$ rad, so according to Eq. (12), the initial desired LOS angle $\lambda_{F0}=3.2015$ rad, which yields $|\lambda_{F0}-\phi_{M0}|=2.4161$ rad $>\pi/2$ rad. To keep the target in the field of the seeker's view, the desired LOS angle λ_F described in Eq. (12) should be modified into the following form:

$$\lambda_F=\phi_T-\tan^{-1}\left(\frac{\sin\theta_{imp}}{\cos\theta_{imp}-V_T/V_M}\right)-\pi \tag{44}$$

The limits of the missile acceleration, the target acceleration and the target acceleration's first time derivative are $A_{M\,max}=200$ m/s^2, $A_{T\,max}=50$ m/s^2 and $\dot{A}_{T\,max}=50$ m/s^3 respectively. The time interval of the simulation is chosen as 0.01 s. Euler algorithm is employed to solve the nonlinear dynamic equations of engagement. The initial values of z_1 and z_2 are set to $V_{\lambda 0}$ and zero respectively. Parameters those are employed for nonsingular terminal sliding surface, reaching law and LESO are as follows: $\beta=10$; $\gamma=1.5$; $\alpha=10/\varepsilon$ and $\omega_0=40$. For constant-maneuvering targets, $\varepsilon=0.1$, $k=120$, $\Delta_\eta=4$. For weaving targets, $\varepsilon=0.05$, $\Delta_\eta=1$, $k=120$ for the frequency of $\pi/10$ rad/s and $k=100$ for the frequency of $\pi/2$ rad/s.

For comparison, the guidance law in [17] is also carried out, where the unknown target acceleration was directly set to zero, i.e., $A_T=0$ m/s^2. The guidance law in [17] is

$$s=(\dot{\lambda}-0)+csign(\lambda-\lambda_F)|\lambda-\lambda_F|^\alpha$$
$$a_m=\frac{\dot{\lambda}}{|\cos(\phi_M-\lambda)|}(cr\alpha\beta|\lambda-\lambda_F|^{\alpha-1}+2|\dot{r}|)+\frac{1}{sign(\cos(\phi_M-\lambda))}\tilde{M}sgmf(s) \tag{45}$$

where $sgmf(s)$ has the same definition as described in Eq. (40), parameters are

$$a=1/\varepsilon,\ \hat{M}=500,\ \varepsilon_M=20,\ \varepsilon_1=0.001,\ \varepsilon_2=0.015,\ \varepsilon=0.2,\ \varepsilon_\lambda=0.0005,\ c=1,\ \alpha=0.5,$$
$$\beta=\begin{cases}0, & |s|<\varepsilon_1\\ \frac{|s|-\varepsilon_1}{\varepsilon_2-\varepsilon_1}, & \varepsilon_1\leq|s|\leq\varepsilon_2\\ 1, & \text{others}\end{cases},\quad \tilde{M}=\begin{cases}\hat{M}, & |s|\geq\varepsilon\\ \frac{\hat{M}}{\varepsilon_M}, & |s|<\varepsilon\end{cases} \tag{46}$$

For simplicity, we denote the guidance laws in this paper and literature [17] as ESONTSM and TSM guidance laws respectively.

Case 1. In this scenario, the target implements a constant maneuver with $A_T=20$ m/s^2, and the simulation results are shown in Fig. 3.

Through the simulation, the actual intercept angles and corresponding intercept times for ESONTSM and TSM guidance laws are 89.9770° and 95.1533°, 17.4 s and 18.21 s, respectively. The ESONTSM guidance law generates a deviation of −0.0230° compared with the desired intercept angle of $\theta_{imp}=90°$, and the

corresponding result under the TSM guidance law is 5.1533°. It can be seen clearly from Fig. 3(b) that the estimation of the unknown target acceleration converges to 19.5 m/s^2 in about 2 s and keeps stable in the interval of 19.9–20.0 m/s^2. Therefore the high estimating precision of the unknown target acceleration can be obtained by using the LESO. It can be observed from Fig. 3(c) that the sliding surface converges rapidly to zero in roughly 10 s under the ESONTSM guidance law, while under the TSM guidance law, it just converges slowly to the boundary layer and keeps there. Fig. 3(d) depicts the trajectories of the LOS angle λ and the desired LOS angle λ_F. In the initial phase, there exists a deviation of 26.5651° between λ and λ_F for both of the ESONTSM and TSM guidance laws. Then it gradually converges to zero in about 12 s under the ESONTSM guidance law and a corresponding value of about 4.11° under the TSM guidance law. In other words, the LOS angle λ tracks the desired LOS angle λ_F in approximately 12 s under the ESONTSM guidance law, while it cannot track that value within the whole phase under the TSM guidance law. The missile acceleration is illustrated in Fig. 3(e), as a result of the constant maneuver of the target, the missile acceleration changes slowly with time under the ESONTSM guidance law, while chattering occurs in the terminal phase under the TSM guidance law.

Case 2. In this scenario, the target implements a constant maneuver with $A_T=30$ m/s^2, and the simulation results are shown in Fig. 4.

Provided $A_{M\ max}=200$ m/s^2, it can be directly observed from Fig. 4(a) that the missile cannot hit the target under the TSM guidance law, while under the ESONTSM guidance law, the impact time is 21.65 s and its corresponding impact angle is 89.9294°. The ESONTSM guidance law yields a deviation of −0.0706° compared with the desired impact angle of $\theta_{imp}=90°$. The reason why the missile misses the target under the TSM guidance law is that the missile cannot provide an enough large acceleration. Hence, the upper constraint of the missile acceleration $A_{M\ max}$ should be improved to avoid missing target. In order to hit the target, $A_{M\ max}$ is increased to 500 m/s^2 under the TSM guidance law. As shown in Fig. 4, the term "TSM500" means the simulation result with $A_{M\ max}=500$ m/s^2 under the TSM guidance law. In this situation, the missile hits the target in 17.64 s and the corresponding intercept angle is 97.2530°. The TSM guidance law generates a deviation of 7.2530° compared with the desired impact angle of $\theta_{imp}=90°$. In Fig. 4(b), the estimation of the target acceleration reaches a value of 29.5 m/s^2 in roughly 1.9 s and then stays in the interval of 29.9 m/s^2 to 30.15 m/s^2, which implies high estimating precision of the target acceleration. In Fig. 4(c), the sliding surface converges to zero quickly in about 3 s under the ESONTSM guidance law, while under the TSM guidance law, it diverges for $A_{M\ max}=200$ m/s^2 and just converges slowly to the boundary layer and keeps there for $A_{M\ max}=500$ m/s^2. In Fig. 4(d), the LOS angle λ tracks the desired LOS angle λ_F in approximately 8 s under the ESONTSM guidance law, while under the TSM guidance law, it diverges for $A_{M\ max}=200$ m/s^2 and reluctantly tracks that value with a deviation of 5.78° for $A_{M\ max}=500$ m/s^2. In Fig. 4(e), the missile acceleration also changes slowly under the ESONTSM guidance law, while under the TSM guidance law, chattering occurs in the terminal stage for $A_{M\ max}=500$ m/s^2. It can be observed from Fig. 4(f) that the TSM guidance law generates a miss distance of 283.4 m for $A_{M\ max}=200$ m/s^2.

Case 3. In this case, consider a weaving target executing sinusoidally varying maneuver. The target acceleration is $A_T=15\sin(\pi/2t)$ m/s^2, and results are shown in Fig. 5.

Under the ESONTSM guidance law, the missile attacks the target in 32.54 s with an impact angle of 90.2709°, while their counterparts under the TSM guidance law are 25.56 s and 92.2367° respectively. Comparing with the desired intercept angle of $\theta_{imp}=90°$, the ESONTSM guidance law generates a deviation of 0.2709°, while a 2.2367° generated under the TSM guidance law. It can be seen from Fig. 5(a) that the target travels along an almost straight line. The reason is that the target's heading angle is a sine function with a magnitude of 2.1885°. In Fig. 5(b), the estimation of the target acceleration tracks the true value in roughly 10 s. In Fig. 5(c), the sliding surface changes quickly under both of the ESONTSM and the TSM guidance laws. It converges to a small neighborhood around zero under the ESONTSM guidance law, but the TSM guidance law cannot achieve this result. In Fig. 5(d), it is obvious that the LOS angle λ tracks the desired LOS angle λ_F in the final stage of guidance under the ESONTSM guidance law, while λ is approximately a constant in the last 8 s of guidance under the TSM guidance law. As pointed out in the introduction that directly setting the unknown target acceleration to zero in designing the sliding surface is equivalent to letting the LOS rate $\dot{\lambda}$ track zero and rendering the LOS angle λ changeless in guidance. But the desired LOS angle λ_F is time-varying when the target executes maneuver, so a changeless LOS angle λ cannot track a time-varying desired LOS angle λ_F. Therefore it can be obviously concluded that simply setting the unknown target acceleration to zero is not reasonable both in theory and simulation. In accordance with the Eq. (42), the estimation of the target acceleration is included in the proposed missile acceleration. That is to say, the missile acceleration will vary similarly as the target acceleration. Therefore in Fig. 5(e), due to the high frequency of the target acceleration, the missile acceleration varies fast under the ESONTSM guidance law.

Case 4. In this case, consider a weaving target executing sinusoidally varying maneuver. The target acceleration is $A_T=15\sin(\pi/10t)$ m/s^2, and results are shown in Fig. 6.

Under the ESONTSM guidance law, the missile hits the target in 22.13 s, while the counterpart under the TSM guidance law is 22.45 s. The impact angles for ESONTSM and TSM guidance laws are 90.0473° and 91.3903° respectively. The corresponding deviations from the desired impact angle of $\theta_{imp}=90°$ are 0.0473° and 1.3903° respectively. It can be seen clearly from Fig. 6(a) that the target's trajectory resembles a wavy line. The reason is that the target's heading angle is a sine function with a magnitude of 10.9427°. In Fig. 6(b), the estimation of the target acceleration tracks the true value in roughly 2.5 s. The sliding surface in Fig. 6(c) converges to zero in about 8 s under the ESONTSM guidance law, while not performs similarly under the TSM guidance law. It can be seen from Fig. 6(d) that the LOS angle λ tracks the desired LOS angle λ_F in about 13 s under the ESONTSM guidance law, while under the TSM guidance law, the LOS angle λ changes slowly in the terminal phase of guidance and therefore cannot track the time-varying desired LOS angle λ_F. The missile acceleration under the ESONTSM guidance law in Fig. 6(e) is smoother than that in Fig. 5(e) due to the lower frequency of the target acceleration. Therefore in order to attack the target with an acceleration of high frequency, it demands higher level of maneuvering capability on missile than that with an acceleration of low frequency. Chattering arises in the TSM guidance law.

So far, four different simulation examples have been implemented to compare the performance of the ESONTSM and TSM guidance laws. All these simulation results are summarized in Table 1.

ESONTSM guidance law can steer missile to attack target in all four cases, while TSM guidance law yields a miss in case 2. In Table 1, the term "none" indicates that the TSM guidance law cannot steer the missile to attack the target with $A_T=30$ m/s^2 and generates a miss distance of 283.4 m when $A_{M\ max}=200$ m/s^2. The term "TSM500" means the TSM guidance law with $A_{M\ max}=500$ m/s^2.

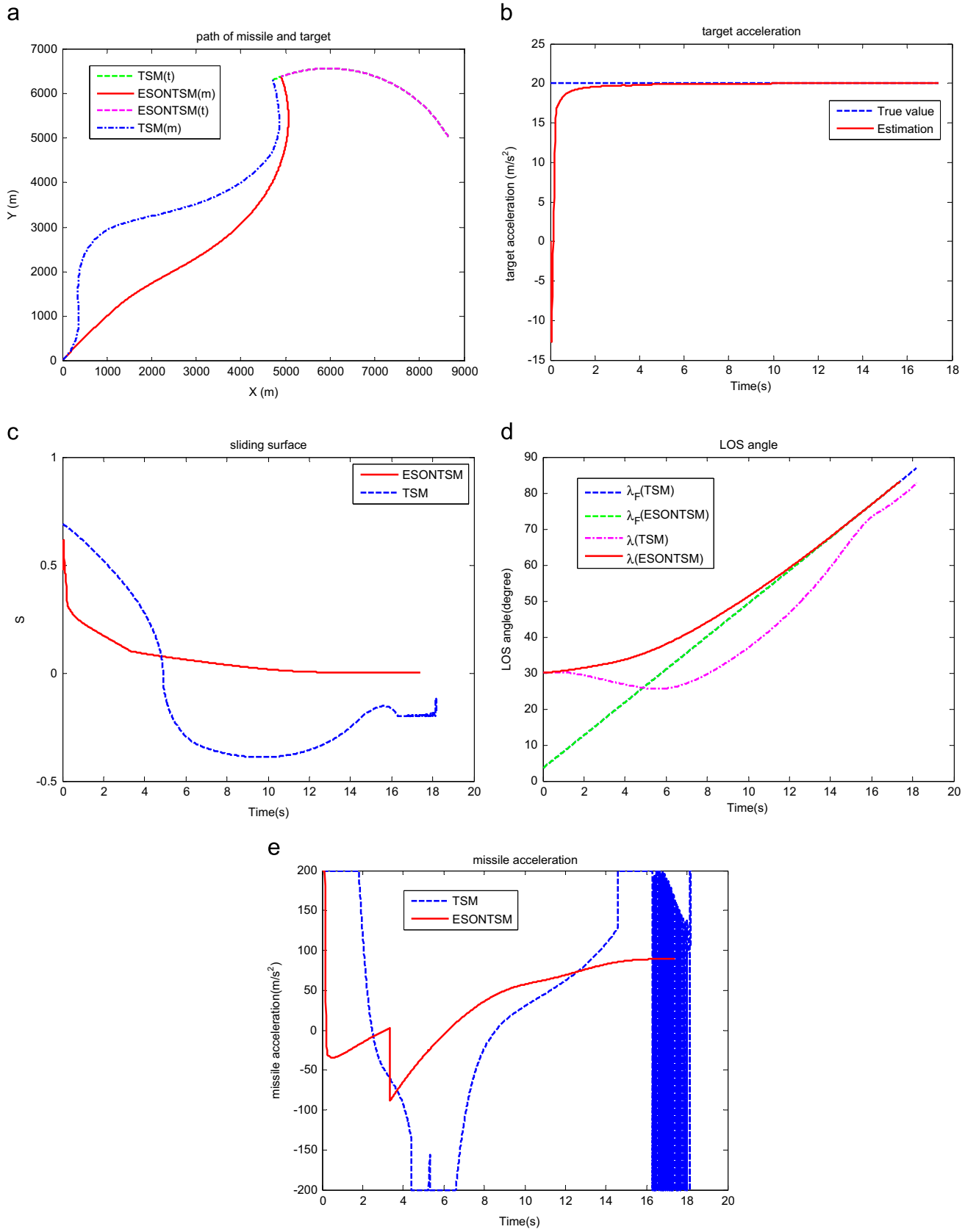

Fig. 3. Results for attacking target with A_T=20 m/s^2: (a) trajectories of missile and target, m and t denote the missile and the target respectively; (b) estimation of the target acceleration; (c) sliding surface; (d) LOS angle and (e) missile acceleration.

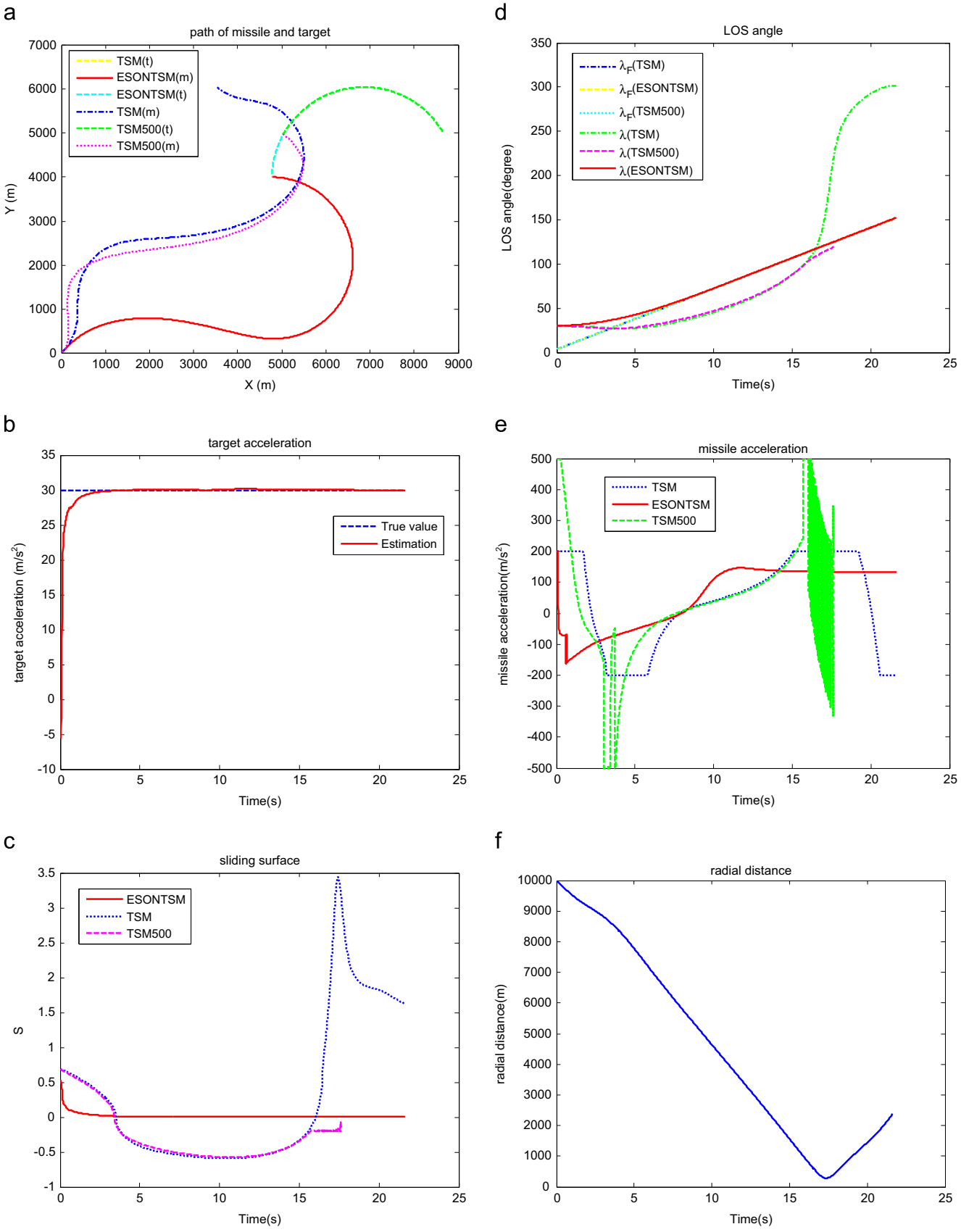

Fig. 4. Results for attacking target with $A_T=30$ m/s^2: (a) trajectories of missile and target, m and t denote the missile and the target respectively; (b) estimation of the target acceleration; (c) sliding surface; (d) LOS angle; (e) missile acceleration and (f) radial distance for TSM guidance law with $A_{M\ max}=200$ m/s^2.

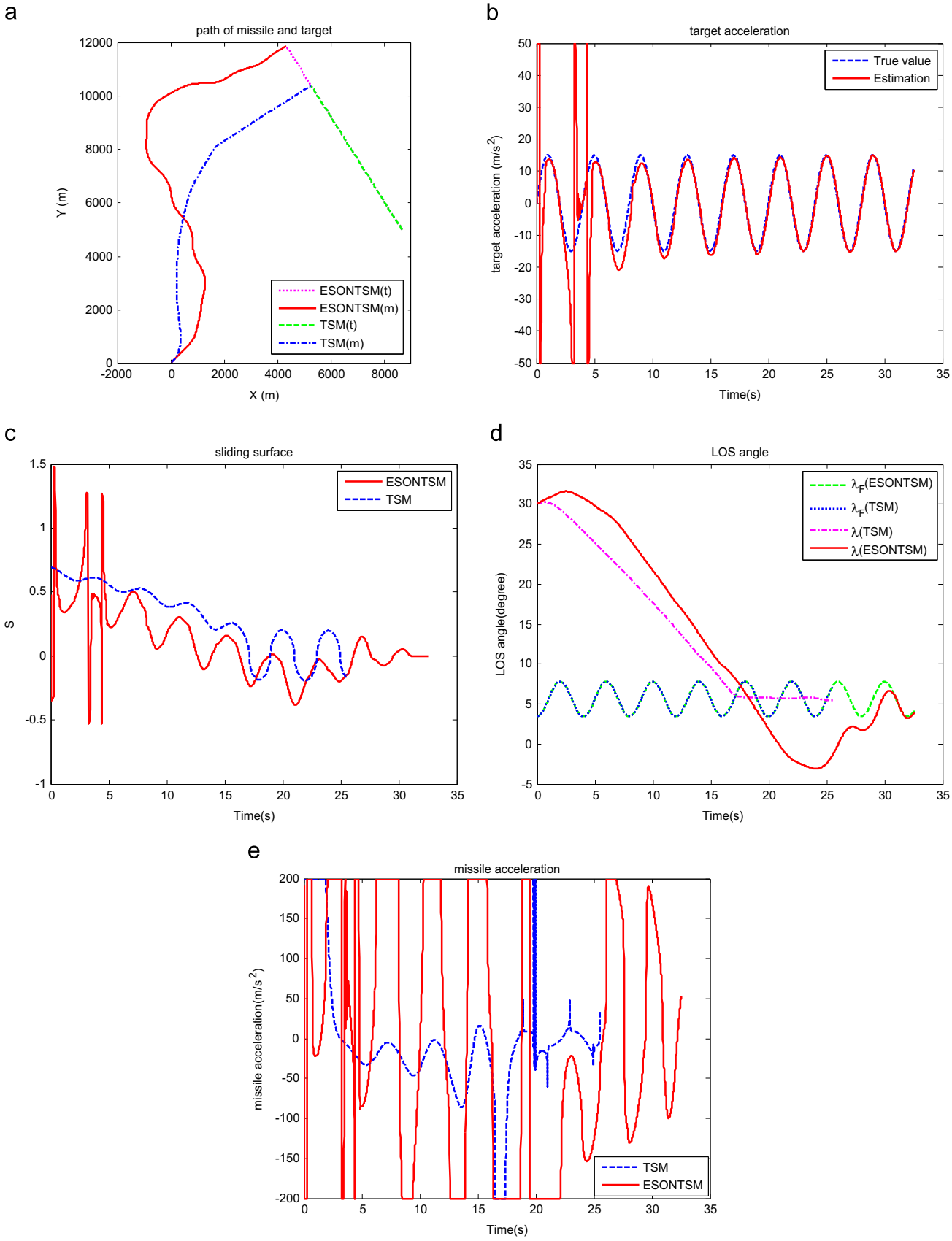

Fig. 5. Results for attacking target with $A_T = 15\sin(\pi/2t)$ m/s^2: (a) trajectories of missile and target, m and t denote the missile and the target respectively; (b) estimation of the target acceleration; (c) sliding surface; (d) LOS angle and (e) missile acceleration.

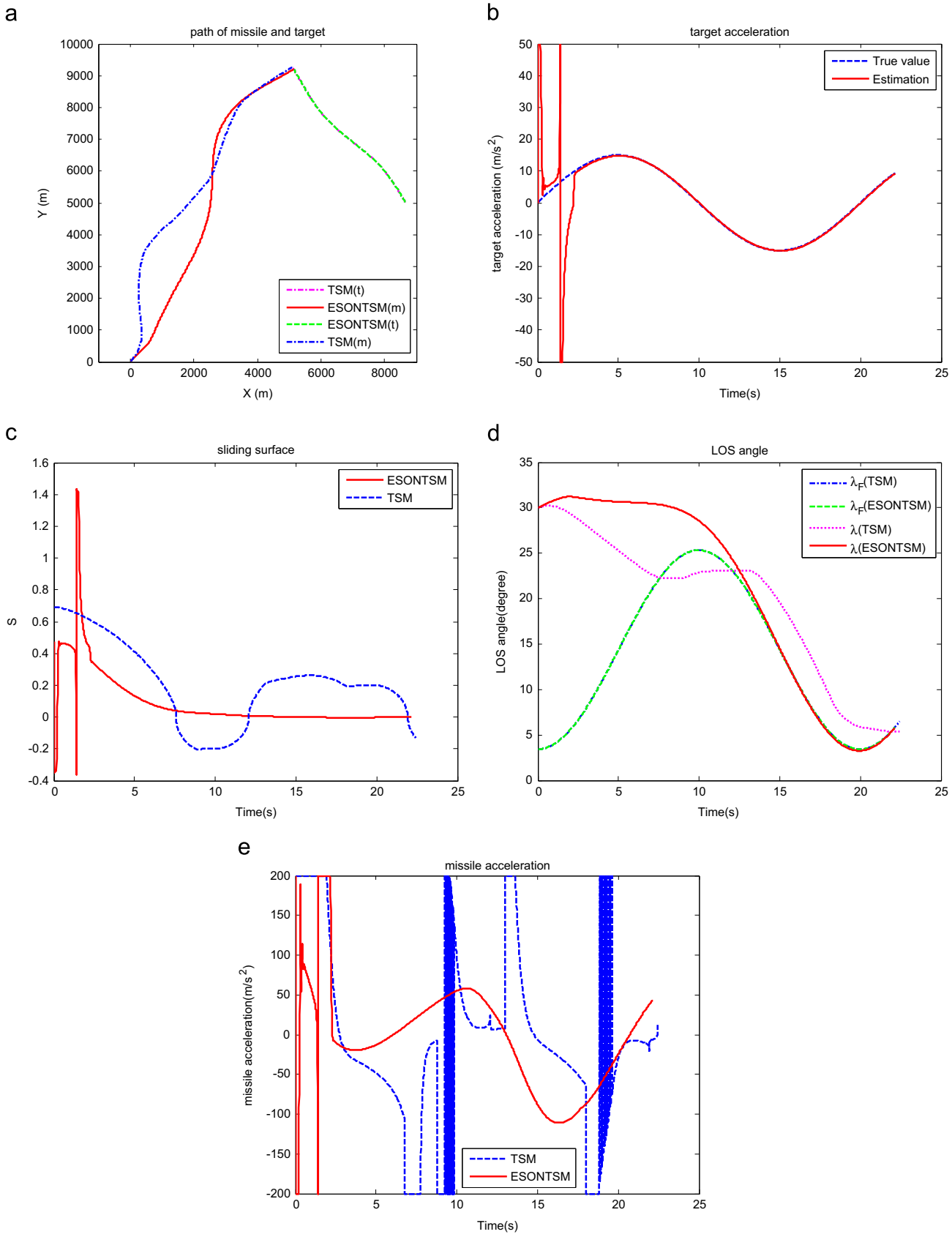

Fig. 6. Results for attacking target with $A_T = 15\sin(\pi/10t)$ m/s^2: (a) trajectories of missile and target, m and t denote the missile and the target respectively; (b) estimation of the target acceleration; (c) sliding surface; (d) LOS angle and (e) missile acceleration.

Table 1
Impact times and intercept angles for four cases.

Target acceleration		20 m/s^2	30 m/s^2	15 sin(πt/2) m/s^2	15 sin(πt/10) m/s^2
Impact time (s)	ESONTSM	17.4	21.65	32.54	22.13
	TSM	18.21	None/17.64(TSM500)	25.56	22.45
Intercept angle (deg)	ESONTSM	89.9770	89.9294	90.2709	90.0473
	TSM	95.1533	None/97.2530(TSM500)	92.2367	91.3903
Deviation (deg)	ESONTSM	−0.023	−0.0706	0.2709	0.0473
	TSM	5.1533	None/7.2530(TSM500)	2.2367	1.3903

In light of this result, two conclusions can be obtained. One is that the ESONTSM guidance law needs a smaller missile acceleration compared with the TSM guidance law. The other is that the requirement of missile acceleration will increase when the maneuvering capability of the target enhanced. Consider Figs. 5(d) and 6 (d), the LOS angle λ is almost changeless in the final stage of guidance. This result proves the theoretical analysis which has been presented in the introduction that setting the unknown target acceleration to zero is equivalent to rendering the LOS angle changeless in guidance. The absolute average of deviations under the ESONTSM and TSM guidance laws are 0.1029° and 4.0083° respectively which generates a difference of about an order of magnitude. Therefore it can be concluded that the proposed guidance law in this paper can achieve higher tracking precision of the desired intercept angle when compared with simply setting the unknown target acceleration to zero.

6. Conclusions

The problem of guidance law design with intercept angle constraint is essentially a problem of state tracking. When attacking maneuvering targets, in order to achieve satisfied tracking performance of the time-varying desired LOS angle, the NTSM control algorithm is employed to design the sliding surface. The LESO is exploited to estimate the unknown target acceleration which is necessary for calculating the designed sliding surface. To demonstrate the superiority of the proposed IAGL, numerical simulations have been implemented for both the traditional TSM guidance law and the proposed guidance law. It has been proved by theoretical analysis and simulation results that the proposed IAGL can achieve higher tracking precision of the desired intercept angle in contrast with the traditional guidance law which simply setting the unknown target acceleration to zero. Future work in this area could focus on developing ESONTSM guidance law with smoother missile acceleration.

Acknowledgments

The authors thank the anonymous reviewers for their many helpful suggestions. The authors are grateful for the projects supported by the National Defense Pre-Research Foundation of China (Grant number B212013XXXX) and the National Natural Science Foundation of China (Grant number 61174094).

References

[1] Kim BS, Lee JG, Han HS. Biased PNG law for impact with angular constraint. IEEE Trans Aerosp Electron Syst 1998;34(1):277–88.
[2] Ratnoo A, Ghose D. Impact angle constrained guidance against nonstationary nonmaneuvering targets. J Guid, Control, Dyn 2010;33(1):269–75.
[3] Lee CH, Kim TH, Tahk MJ. Interception angle control guidance using proportional navigation with error feedback. J Guid, Control, Dyn 2013;36(5):1556–61.
[4] Zhang YA, Ma GX, Liu AL. Guidance law with impact time and impact angle constraints. Chin J Aeronaut 2013;26(4):960–6.
[5] Song TL, Shin SJ, Cho HJ. Impact angle control for planar engagements. IEEE Trans Aerosp Electron Syst 1999;35(4):1439–44.
[6] Ryoo CK, Cho HJ, Tahk MJ. Time-to-go weighted optimal guidance with impact angle constraints. IEEE Trans Control Syst Technol 2006;14(3):483–92.
[7] Lee CH, Tahk MJ, Lee JI. Generalized formulation of weighted optimal guidance laws with impact angle constraint. IEEE Trans Aerosp Electron Syst 2013;49(2):1317–22.
[8] Utkin V. Variable structure systems with sliding modes. IEEE Trans Autom Control 1977;22(2):212–22.
[9] Shafiei MH, Binazadeh T. Application of partial sliding mode in guidance problem. ISA Trans 2013;52(2):192–7.
[10] Shafiei MH, Binazadeh T. Partial stabilization-based guidance. ISA Trans 2012;51(1):141–5.
[11] Moon J, Kim K, Kim Y. Design of missile guidance law via variable structure control. J Guid, Control, Dyn 2001;24(4):659–64.
[12] Shtessel YB, Shkolnikov IA, Levant A. Smooth second-order sliding modes: missile guidance application. Automatica 2007;43(8):1470–6.
[13] Shima T. Intercept-angle guidance. J Guidance, Control, Dyn 2011;34(2):484–92.
[14] Harl N, Balakrishnan SN. Impact time and angle guidance with sliding mode control. IEEE Trans Control Syst Technol 2012;20(6):1436–49.
[15] Zhang YX, Sun MW, Chen ZQ. Finite-time convergent guidance law with impact angle constraint based on sliding-mode control. Nonlinear Dyn 2012;70(1):619–25.
[16] Zhang ZX, Li SH, Luo S. Composite guidance laws based on sliding mode control with impact angle constraint and autopilot lag. Trans Inst Meas Control 2013;35(6):764–76.
[17] Kumar SR, Rao S, Ghose D. Sliding-mode guidance and control for all-aspect interceptors with terminal angle constraints. J Guid, Control, Dyn 2012;35(4):1230–46.
[18] Kumar SR, Rao S, Ghose D. Non-singular terminal sliding mode guidance and control with terminal angle constraints for non-maneuvering targets. In: Proceedings of the 12th international workshop on variable structure systems; 2012. p. 291–6.
[19] Zheng Z, Dong X, Liu JM, Xia YQ. Missile guidance law based on extended state observer. IEEE Trans Ind Electron 2013;60(12):5882–91.
[20] Feng Y, Yu XH, Man ZH. Non-singular terminal sliding mode control of rigid manipulators. Automatica 2002;38(12):2159–67.
[21] Yu SH, Yu XH, Shirinzadeh B, Man ZH. Continuous finite-time control for robotic manipulators with terminal sliding mode. Automatica 2005;41(11):1957–64.
[22] Han JQ. A class of extended state observers for uncertain systems. Control Decis 1995;10(1):85–8 (in Chinese).
[23] Huang Y, Han JQ. Analysis and design for the second order nonlinear continuous extended state observer. Chin Sci Bull 2000;45(21):1938–44.
[24] Han JQ. From PID to active disturbance rejection control. IEEE Trans Ind Electron 2009;56(3):900–6.
[25] Zheng Q, Gao LQ, Gao ZQ. On stability analysis of active disturbance rejection control for nonlinear time-varying plants with unknown dynamics. In: Proceedings of the 46th IEEE conference on decision and control; 2007. p. 3501–6.
[26] Zheng Q, Gao LQ, Gao ZQ. On validation of extended state observer through analysis and experimentation. J Dyn Syst, Meas, Control – Trans ASME 2012;134(2):024505 (6 pages).
[27] Guo BZ, Zhao ZL. On the convergence of an extended state observer for nonlinear systems with uncertainty. Syst Control Lett 2011;60(6):420–30.
[28] Gao ZQ. Scaling and bandwidth-parameterization based controller tuning. In: Proceedings of the 2003 American control conference; 2003. p. 4989–96.
[29] Gao ZQ. Active disturbance rejection control: a paradigm shift in feedback control system design. In: Proceedings of the 2006 American control conference; 2006. p. 2399–405.
[30] Goforth FJ, Zheng Q, Gao ZQ. A novel practical control approach for rate independent hysteretic systems. ISA Trans 2012;51(3):477–84.
[31] Dong LL, Edwards J. Active disturbance rejection control for an electrostatically actuated MEMS device. Int J Intell Control Syst 2011;16(3):160–9.